Semiconductors, 2023, Vol. 57, No. 9

Gunn generation mode in a resonator based on an array of ordered carbon nanotubes (CNTs)

© I.O. Zolotovskii[1], A.S. Kadochkin[1], I.S. Panyaev[1], I.A. Rozhleys[1,2], D.G. Sannikov[1]

[1] Ulyanovsk State University,
432009 Ulyanovsk, Russia
[2] „System Integration“ Company,
119971 Moscow, Russia

E-mail: sannikov-dg@yandex.ru

Received July 1, 2023
Revised November 20, 2023
Accepted December 11, 2023

We find and study the generation regime of microwave waves in a model resonator cavity based on an array of ordered semiconductor carbon nanotubes. Within the framework of the phenomenological approach, the Gunn effect was discovered for aligned carbon nanotubes with a length of $25-150\,\mu$m, the influence of the main parameters (changes in the electric field, the distance between the electrodes, the voltage at the contacts, etc.) was studied and it was shown that the electronic efficiency during lasing can reach 13%. The results obtained can be used to design new resonator structures such as compact microwave amplifiers and emitters based on ordered arrays of nanotubes.

Keywords: Gunn effect, carbon nanotube (CNT), resonator, generation.

DOI: 10.61011/SC.2023.09.57436.5381

1. Introduction

Traditional Gunn Diodes (GD) — these are semiconductor devices with negative differential resistance arising in a homogeneous semiconductor crystal (for example, n-GaAs, GaN, InP, etc., etc.) when a strong electric field is applied to it [1,2]. GD are used to generate and amplify electric oscillations of the microwave range. Depending on the parameters of the crystal, load, supply voltage and temperature, the GD can operate in one of the modes: domain (which is divided into span, delayed domain formation and domain quenching); hybrid; limited space-charge accumulation (or stable gain mode) and negative conductivity [3]. The generation mode is largely determined by the product of the concentration of the dopant n by the crystal length l, i.e. $n \cdot l$. Commercially available GD are designed to amplify and generate radiation at frequencies from $1-2$ to 150 GHz or more. At the same time, their output power in continuous mode ranges from units of milliwatts in the upper microwave region to units of watts in the decimeter and meter ranges. Increased output power values for all modes, except for the limited space-charge accumulation mode, are obtained by increasing the operating current of the diode, which in turn requires an increase in the cross-sectional area of the crystal and an improvement in heat dissipation. For frequencies < 1 GHz, microwave transistors with much better functionality are used. The main difficulties in studying the operation of GD are a detailed understanding of the process of domain nucleation with different doping profiles, as well as the features of multi-domain formation.

It was noted [4] in 2000s that the Gann effect can occur due to the existence of a region of negative differential resistance (NDR) (or negative conductivity) in graphene structures — semiconductor single-walled carbon nanotubes (CNTs). Depending on the twist angle of the graphene sheet described by the chirality indices (n, m), CNTs can be metallic (if the difference $n - m$ is divisible by 3) or semiconductor (with others n and m). Experimentally, NDR was detected in single and multi-wall CNTs [5–12], as a rule, when measuring volt-ampere characteristics. Sites with n- or p-type of conductivity were obtained in early work [5] in a single-wall semiconductor CNT by changing the degree of doping, which led to the occurrence of NDR at low temperatures (up to 180 K). It was later demonstrated that a CNT-based field-effect transistor shows NDR at 300 K [11]. The so-called „suspended“ metal single-wall CNTs located above the gate also detect NDR [6], which is proposed to be used to create gas sensors based on field-effect transistors (suspended CNT-FET) [13]. The possibility of implementing NDR in single-walled CNTs was experimentally shown in the work [7], where NDR was observed in tunnel spectra recorded on atomic defects of hydrogen and nitrogen in semiconductor-type CNTs, and, presumably, was associated with defective electronic states in the band gap. The authors of [10] point the formation of $p-n$ transitions (quantum dots) in the midpoint of single-walled CNTs due to the recharge of islands of atomic layered deposition, whose resonant tunneling levels make the phenomenon of NDR possible. NDR can also be associated with the high photoconductivity of the tube, which plays the role of a gate [8]. NDR was observed in article [9] in multi-walled CNTs (up to 17 nm in

diameter). Presumably, the cause of the NDR was interlayer resonant tunneling. In a recent article [12], the same authors discovered areas of NDR during conductivity measurements in semiconductor multilayer CNTs (diameter 2.5–10 nm) synthesized by arc discharge. The origin of NDR in CNT systems (in contrast to the traditional NDR mechanism associated with the interline electronic transition in n-GaAs) may be associated with the effects of band structure, phonon blockade, chemical reactions, temperature control, electrical contacts, mechanical deformations [14–16]. The creation of vertical and horizontal aligned carbon nanotube arrays [17–21], as well as record values of constitutive parameters and kinetic coefficients of CNTs, allows to hope for the implementation of Gunn generation, which differs from the traditional one arising in GaAs, InP and other materials.

The possibility of amplification and obtaining a controlled mode of microwave generation in a resonator cavity filled with an array of ordered semiconductor CNTs is considered in this article. The review is carried out within the framework of a quasi-one-dimensional model.

2. Problem statement and model

Consider a resonator filled with identical semiconductor CNTs located parallel to the axis x from the anode to the cathode. Note that in order to preserve the semiconductor properties, CNTs should have a small diameter (< 10 nm) [9,12,22]. A constant electric field E_0 is applied to the electrodes and directed along the axis x (Figure 1).

We will describe the physical processes in the resonator using a quasi-one-dimensional model of the Gann diode, assuming that the structure has the shape of a circle with a diameter d in the plane yz. Assuming that charges (electrons) move in the same direction from the cathode to the anode in the CNT structure, we will consider the current density j and the electric field E in the cross-sectional plane unchanged. The problem is simplified with such assumptions, and the Poisson equations and the total current (consisting of conduction currents j_{cond}, diffusion j_{diff} and displacement j_{displ}) become one-dimensional (see, for example, [1,3]):

$$\varepsilon\varepsilon_0 \frac{\partial E}{\partial x} = \rho = e[n(x,t) - N_D], \tag{1}$$

$$j = j_{\text{cond}} + j_{\text{diff}} + j_{\text{displ}} = env - eD\nabla n + \varepsilon\varepsilon_0 \frac{\partial E}{\partial t}. \tag{2}$$

Here ε_0 and ε — dielectric permittivity of vacuum and interelectrode medium (array of ordered CNTs), e and n — electron charge and concentration, N_D — donor concentration, $\rho(x,t)$, $E(x,t)$, $v(x,t)$ — volumetric density of an external electric charge, electric field strength and drift velocity of directional carrier motion, respectively; D — diffusion coefficient.

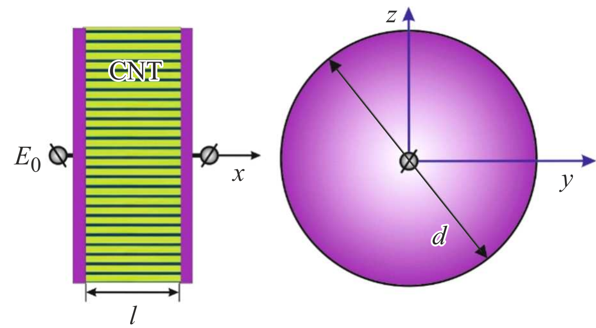

Figure 1. Geometry of a resonator filled with CNT.

The equation of the total current density

$$\frac{\partial j}{\partial x} = 0, \tag{3}$$

therefore, taking into account the above relations, we obtain the equation for the electric field:

$$\frac{i_a}{\varepsilon A} - \frac{e}{\varepsilon} n_0 v(E) - v(E)\frac{\partial E}{\partial x} - \frac{\partial E}{\partial t} + D\frac{\partial^2 E}{\partial x^2} + \frac{e}{\varepsilon} D \frac{\partial n_0}{\partial x} = 0, \tag{4}$$

where i_a — (anode) the current of the external circuit, n_0 — the concentration of electrons at the initial time. The initial condition (at time $t = 0$) is based on the assumption of equality of drift and diffusion currents, from

$$E(x) = \varphi_T \frac{1}{N_D}\frac{\partial N_D}{\partial x}, \tag{5}$$

where $\varphi_T = D/\mu_n$ — temperature potential (Einstein ratio), μ_n — electron mobility. If the diode contacts (cavities) are well conductive, then there is practically no voltage drop on them and the electric field strength is close to zero. Then the boundary conditions take the following form

$$E(x = 0, t) = 0,$$
$$E(x = l, t) = 0. \tag{6}$$

Anode current

$$i_a = \left(U_0 - \int_0^l E dx\right)/Rn,$$

where R — load resistance, U_0 — contact voltage. We use an approximation of the dependence of the electron drift velocity on the electric field for semiconductor CNTs, given in the article [23]:

$$v(E) = \left[\mu_n E + v_{\text{sat}}\left(\frac{E}{E_m}\right)^2\right] \Big/ \left[1 + \frac{\mu_n E}{v_{\text{fit}}} + \left(\frac{E}{E_m}\right)^2\right]. \tag{7}$$

This dependence is constructed for the following parameters In Figure 2: $\mu_n = 7.9\,\text{m}^2/(\text{V}\cdot\text{s})$ — electron mobility in semiconductor CNTs [24], $v_{\text{sat}} = 3 \cdot 10^5$ m/s — saturation

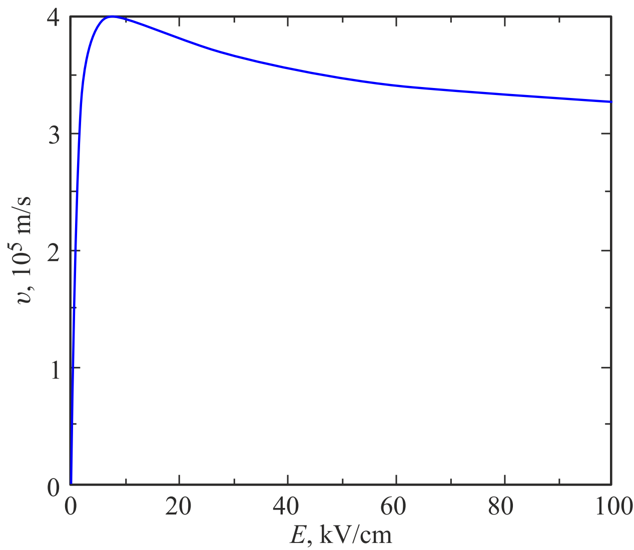

Figure 2. Approximation of the dependence of the electron drift velocity on the electric field in semiconductor CNTs [23].

rate, and $v_{\text{fit}} = 5 \cdot 10^5$ m/s and $E_m = 4 \cdot 10^5$ V/m — fitting parameters. At the same time, the saturation rate is $\sim 1/3$ the Fermi velocity in graphene and practically does not depend on the CNT diameter [23]. The differential electron mobility $\mu_d = \frac{dv}{dE}$ becomes negative starting from ~ 10 kV/cm, which determines the possibility of Gunn generation.

Let's evaluate the conditions under which the domain mode is implemented in the structure under consideration. It is known [25] that the domain has time to form if the time of flight from the cathode to the anode is $t_{sp} = l/v_{\max}$ ($v_{\max}$ — the maximum drift velocity of the carriers) will be significantly longer than the rise time of a small fluctuation

$$t_{gr} \cong 3\tau_{md} = \frac{3\varepsilon\varepsilon_0}{en_0|\mu_d|},$$

where l — distance between electrodes, τ_{md} — Maxwell relaxation time (domain resorption). This condition leads to the so-called Kremer criterion:

$$n_0 l \geq \frac{3\varepsilon\varepsilon_0 v_{\max}}{e|\mu_d|}. \tag{8}$$

On the other hand, carrier diffusion should not noticeably reduce the increase in fluctuations, which occurs when the characteristic diffusion time $\tau_D \approx l^2/4\pi^2 D$ (D —diffusion coefficient) is longer than the time τ_{md}. It is taken into account here that the wavelength of the 1st harmonic is equal to the length of the sample. As a result, we come to an expression for the parameter $n_0 l^2$, which defines the lower limit of the Gunn generation:

$$n_0 l^2 \geq 4\pi^2 \varepsilon_0 \varepsilon D/e|\mu_d|. \tag{9}$$

In general, the diffusion coefficient may depend on the field, i.e. $D = D(E)$, however, taking this dependence into account in GaAs-GD does not lead to new results [3].

Conditions (7) and (8) give expressions for the lengths defining the limits of the generation mode:

$$l_{\min} = 2\pi\sqrt{\frac{\varepsilon D}{e|\mu_d|n_0}}, \quad l_{\max} = \frac{3\varepsilon\varepsilon_0 v_{\max}}{e|\mu_d|n_0}. \tag{10}$$

Note that this model works correctly if the electron acceleration length is much less than the cavity length l.

3. Numerical analysis and discussion

For numerical analysis, the values corresponding to the real CNT parameters are selected. In experimental work [26–28], the electron diffusion coefficient in multilayer CNTs was determined, the values of which lie in the range from 0.01 to 0.09 m^2/s. We assume the coefficient $D = 0.036$ m^2/s in calculations, which falls within the specified range and corresponds to the value typical for graphene [29]. The actual part of the dielectric constant ε' of the microwave region can vary widely due to changes in the volume fraction and composition of CNTs in the matrix [30,31]. By choosing the value $\varepsilon' \approx 6$, we can neglect the losses in the system, considering the imaginary part of the dielectric function small ($\varepsilon'' \ll \varepsilon'$). At the same time, the maximum value of differential mobility is $|\mu_d| \approx 2 \cdot 10^{-2}$ m^2/(V $\cdot$ s) [23], and the average concentration of donor impurities is of the order of $n_0 \approx 10^{21}$ m^{-3} [32].

We assume that the CNT doping profile at the initial time has the form shown in Figure 3. A similar profile can be created, for example, by adsorbing potassium or bromine atoms [33–35] onto the CNT surface. The „depression" concentrations may be due to doping heterogeneity, field fluctuations, or thermal fluctuations [36]. This doping profile is repeated (in percentage terms) for any selected

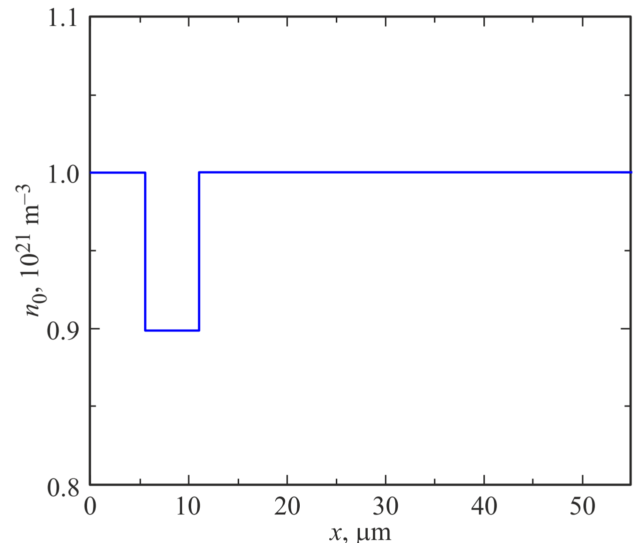

Figure 3. Distribution of the concentration of donor impurities at time $t = 0$, length $l = 55\,\mu$m.

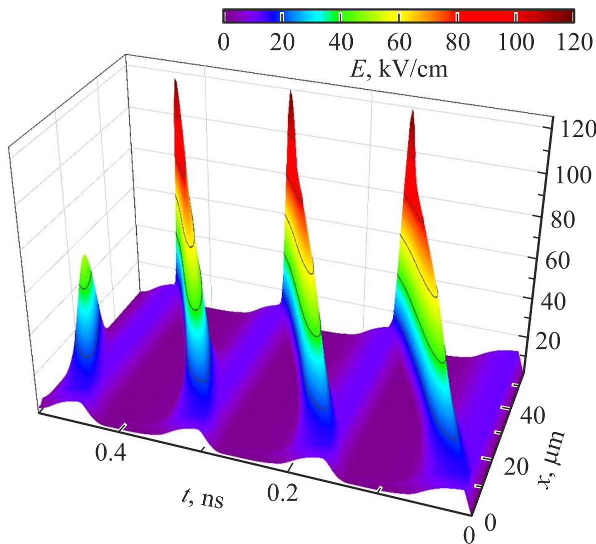

Figure 4. Space-time dependences of the electric field in the CNT resonator with the parameters: length $l = 55\,\mu$m, cavity diameter $d = 50\,\mu$m, applied voltage $U_0 = 70$ V, load resistance $R = 10$ Ohms, initial electron concentration in CNT $n_0 = 10^{21}\,\mathrm{m}^{-3}$ [32]. The domain generation mode is implemented. (The colored version of the figure is available on-line).

length l GD and is described by a piecewise given function in which the step is removed from the beginning (cathode) by 1/10 of the entire length l.

Figure 4 shows a picture of the development of domain instability in the resonator, based on the solution of the equation (4) by the finite element method. The rise time t_1 of the voltage U_0 is small compared to the voltage retention time ($t_1 \ll t_2$). Figure 4 shows that domains occur in the simulated resonant cavity with a period of ~ 0.15 ns and their transit-time frequency f_{sp} is ~ 7 GHz, which is consistent with the estimate $f_{sp} \approx v_{\max}/l$, where $v_{\max}$ — the maximum drift velocity of electrons. The peak value of the electric field exceeds 100 kV/cm, which is almost an order of magnitude higher than the applied voltage $E = U_0/d \approx 12$kV/cm. Note that a similar relationship is observed in traditional GD based on n-GaAs [2].

The pre- and post-domain modes and the Gunn generation mode are shown in Figure 5. It should be noted that, according to (9), the estimated values of the boundary lengths of the resonator are $l_{\min} \approx 5.2\,\mu$m and $l_{\max} \approx 22.4\,\mu$m, then the calculation gives the lengths $l_{\min} = 25$ um (a), $l = 55$ um (b) and $l_{\max} \approx 150$ um (c). This may be due to the difference in the mechanisms of occurrence of NDR

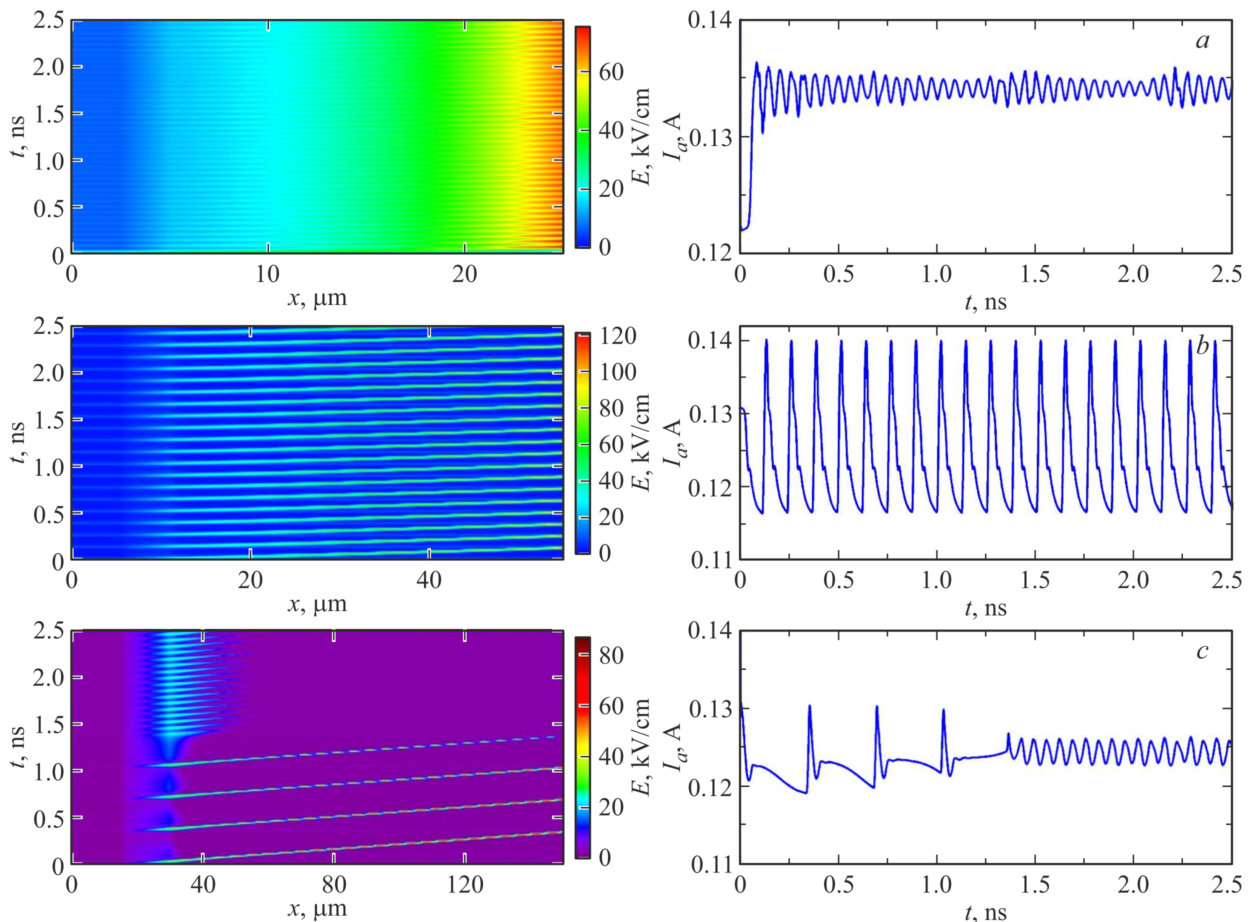

Figure 5. The space-time distribution of the electric field and the corresponding ampere-time characteristics in the initial stage of the domain mode (a), during generation (b) and in the final stage of the domain mode (c). Modes occur for different cavity lengths $l_{\min} = 25\,\mu$m (a), $l = 55\,\mu$m (b) and $l_{\max} = 150\,\mu$m (c). The remaining parameters are the same as for Figure 4.

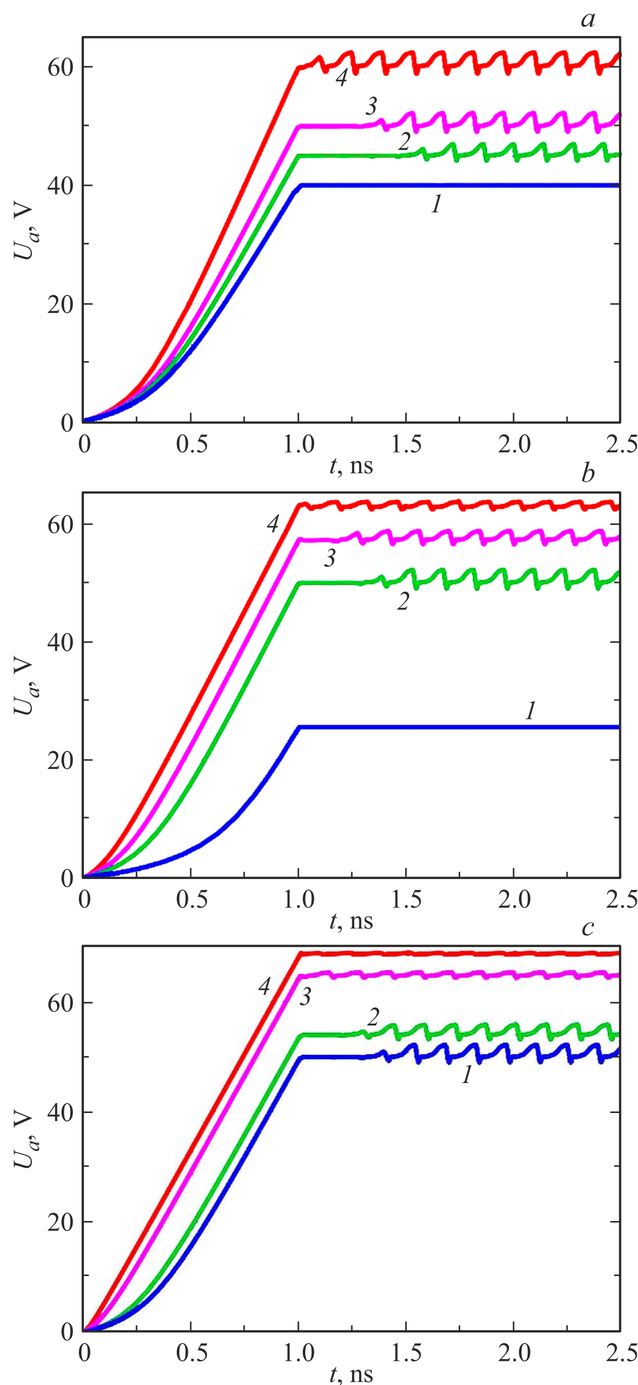

Figure 6. Dependences of the anode voltage on the DC on time ($l = 55\,\mu$m): a — for different values of bias voltages $U_0 = 60$, 65, 70, 80 V (curves *1–4*), $d = 50\,\mu$m, $R = 150$ Ohm; b — for different cross sections, i.e. values $d = 75$, 50, 40, 30 μm (curves *1–4*). $U_0 = 70$ V, $R = 150$ Ohms; c — for different load resistance values $R = 150$, 120, 40, 10 Ohms (curves *1–4*). $U_0 = 70$ V, $d = 50\,\mu$m. Signal rise time $t_1 = 1$ ns.

in CNT and GaAs noted in the Introduction. In addition, the boundaries of the domain mode can be significantly affected by the initial concentration distribution (doping profile) $n_0(x)$ [3].

Dependence of the Gunn generation frequency on the resonator length*

l, μm	35	45	55	60
f, GHz	–	8.7	7.1	6.4

Note. * Parameters $U_0 = 70$ V, $d = 50\,\mu$m, $R = 150$ Ohms.

Figure 6 shows the dependences of the anode voltage on the time on GD for different values of offset voltages (a), diameter (b) and load resistance (c). It is known that the frequency of traditional Gunn generators is weakly dependent on the applied voltage. With an increase in the applied voltage, the thickness of the domain increases slightly, while the speed of its movement changes slightly. A decrease of the load resistance leads to an increase of the amplitude of the variable part of the output signal (curves *2–4* in Figure 6, c). Note that the generation mode starts earlier for higher voltage values U_0 (Figure 6, a), smaller diameter values d (Figure 6, b), and lower load resistance values R (Figure 6, c). In addition, we estimated the frequency of the Gunn generation from the length of the resonator. As can be seen from the table, generation occurs in cavities with a length of $l > 35\,\mu$m, and the generation frequency decreases with the increase of the resonator length.

Figure 7 shows the dependence of the average electronic efficiency $\eta = P/P_{\text{out}}$ on the voltage at the resonator. The power consumption and output were determined as follows: $P = I_0U_0$, $P_{\text{out}} = I_aU_a$, with I_0 and I_a — the consumed and output (anode) currents, U_0 and U_a — applied and output (anode) voltages. As can be seen from Figure 7, the electronic efficiency increases with the decrease of voltage

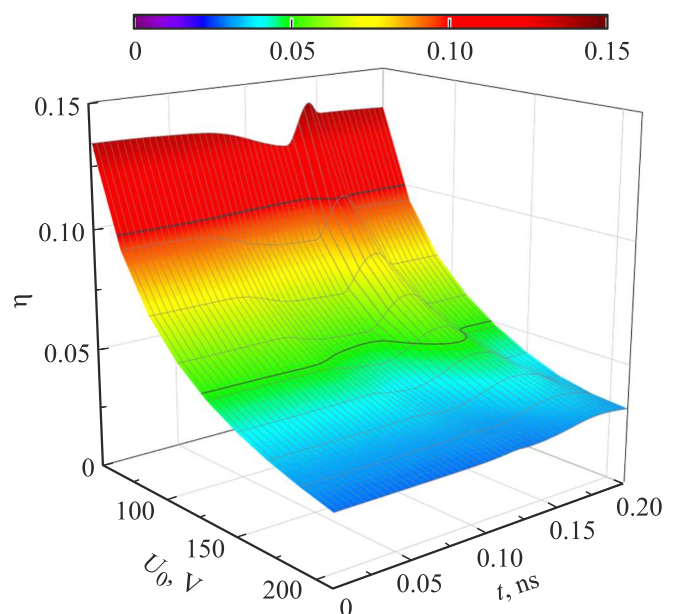

Figure 7. Dependence of the average electronic efficiency on the voltage at the resonator. Parameters are same as in Figure 4.

on the GD, reaching a value of $\sim 13\%$, which exceeds the electronic efficiency ($1-5\%$, [3]) of modern GDs on based on GaAs. Additional analysis shows that there is a limit value of $R_{\max}$ at which the generation stops. For this set of parameters (see Figure 7) $R_{\max} = 227$ Ohms.

4. Conclusion

Thus, we discovered and investigated the Gunn generation mode of ultrahigh frequency radiation in a resonant cavity filled with CNT. The possibility of controlling the microwave generation process by changing external parameters (applied voltage, load resistance) and internal parameters (length and diameter of the cavity) is demonstrated using the finite element modeling. It was found that the maximum generation frequencies correspond to small resonator lengths, and the values of resonator lengths predicted by the standard theory do not correspond to the calculated ones. It is shown that the electronic efficiency for a CNT resonator can reach values of 13%, which exceeds the electronic efficiency ($1-5\%$ in continuous mode) of modern GaAs-based GDs. It is preferable to use horizontally oriented CNT arrays for the experimental implementation of the proposed scheme, which are usually grown on flat substrates and parallel to the substrate, with large distances between the tubes. They are up to centimeters and even decimeters long, and their aspect ratio can exceed 10^6-10^8. Individual CNT in the array have $1-5$ shells and a small diameter ($1-5$ nm). The interactions between the tubes are weak, which leads to a relatively low defect density [17,18]. The number of CNTs in the array should be such that the current distribution over the CNTs does not exceed the limits of several microamps per tube, since otherwise the resistance of the CNTs increases significantly [37]. Electrodes made of highly conductive metals can be used as contacts: silver (Au) [38], nickel (Ni) and silver (Au) [5], gold (Au) [39], titanium (Ti) and platinum (Pt), palladium Pd [40], etc., providing a heat sink to maintain a constant temperature. Resistance of contact „metal–CNT" is determined by the parallelism and uniformity of CNTs in the array [41]. Metal catalysts (for example, Fe, Co, Ni) deposited on the ends of CNTs before obtaining external metallization tracks, as well as thermal annealing in the presence of a transition metal can be used to improve the contact properties [42].

The results obtained can also be used in radiophotonics and optical communication in the development of compact microwave amplifiers and generators.

Funding

The study was funded by a grant from the Russian Science Foundation (project No. 23-19-00880) and with support by a grant of the Ministry of Science and Higher Education of the Russian Federation (No. 075-15-2021-581).

Conflict of interest

The authors declare that they have no conflict of interest.

References

[1] D.P. Tsarapkin. *Generatory SVCH na diodakh Ganna* (M., Radio i svyaz', 1982). (in Russian).

[2] M.E. Levinstein, Yu.K. Pozhela, M.S. Shur. *Gunn Effect* (M., Sov. radio, 1975). (in Russian).

[3] G.I. Veselov. *Mikroelektronnye ustrojstva SVCH* (M., Vyssh. shk., 1988). (in Russian).

[4] A.S. Maksimenko, G.Y. Slepyan. Phys. Rev. Lett., **84**, 362 (2000). https://doi.org/10.1103/PhysRevLett.84.362

[5] C. Zhou, J. Kong, E. Yenilmez, H. Dai. Science, **290**, 1552 (2000). https://doi.org/10.1126/SCIENCE.290.5496.1552

[6] E. Pop, D. Mann, J. Cao, Q. Wang, K. Goodson, H. Dai. Phys. Rev. Lett., **95**, 155505 (2005). https://doi.org/10.1103/PhysRevLett.95.155505

[7] G. Buchs, P. Ruffieux, P. Gröning, O. Gröning. Appl. Phys. Lett., **93**, 073115 (2008). https://doi.org/10.1063/1.2975177/336360

[8] S.W. Lee, A. Kornblit, D. Lopez, S.V. Rotkin, A.A. Sirenko, H. Grebel. Nano Lett., **9**, 1369 (2009). https://doi.org/10.1021/nl803036a

[9] M. Ahlskog, O. Herranen, A. Johansson, J. Leppäniemi, D. Mtsuko. Phys. Rev. B, **79**, 155408 (2009). https://doi.org/10.1103/PhysRevB.79.155408

[10] M. Rinkiö, A. Johansson, V. Kotimaki, P. Törmä. ACS Nano, **4**, 3356 (2010). https://doi.org/10.1021/nn100208v

[11] K.A. Shah, M.S. Parvaiz. Superlatt. Microstruct., **100**, 375 (2016). https://doi.org/10.1016/J.SPMI.2016.09.037

[12] M. Ahlskog, O. Herranen, J. Leppäniemi, D. Mtsuko. Eur. Phys. J. B, **95**, 130 (2022). https://doi.org/10.1140/EPJB/S10051-022-00392-Z

[13] S. Jung, R. Hauert, M. Haluska, C. Roman, C. Hierold. Sensors Actuators B: Chem., **331**, 129406 (2021). https://doi.org/10.1016/J.SNB.2020.129406

[14] T.D. Yuzvinsky, W. Mickelson, S. Aloni, G.E. Begtrup, A. Kis, A. Zettl. Nano Lett., **6**, 2718 (2006). https://doi.org/10.1021/nl061671j

[15] S. Choudhary, G. Saini, S. Qureshi. Mod. Phys. Lett. B, **28**, 1450007 (2014). https://doi.org/10.1142/S0217984914500079

[16] S.A. Evlashin, M.A. Tarkhov, D.A. Chernodubov, A.V. Inyushkin, A.A. Pilevsky, P.V. Dyakonov, A.A. Pavlov, N.V. Suetin, I.S. Akhatov, V. Perebeinos. Phys. Rev. Appl., **15**, 054057 (2021). https://doi.org/10.1103/PhysRevApplied.15.054057

[17] R. Zhang, Y. Zhang, F. Wei. Chem. Soc. Rev., **46**, 3661 (2017). https://doi.org/10.1039/C7CS00104E

[18] M. He, S. Zhang, J. Zhang. Chem. Rev., **120**, 12592 (2020). https://doi.org/10.1021/ACS.CHEMREV.0C00395

[19] L. Liu, J. Han, L. Xu, J. Zhou, C. Zhao, S. Ding, H. Shi, M. Xiao, L. Ding, Z. Ma, C. Jin, Z. Zhang, L.M. Peng. Science, **368**, 850 (2020). https://doi.org/10.1126/science.aba5980

[20] S. Shekhar, P. Stokes, S.I. Khondaker. ACS Nano, **5**, 1739 (2011). https://doi.org/10.1021/nn102305z

[21] J. Kimbrough, L. Williams, Q. Yuan, Z. Xiao. Micromachines, **12** (1), 12 (2021). https://doi.org/10.3390/MI12010012

[22] M.J. Biercuk, S. Ilani, C.M. Marcus, P.L. McEuen. *Electrical transport in single-wall carbon nanotubes* (In: Topics Appl. Phys., Springer, Berlin, Heidelberg, 2008) p. 455. https://doi.org/10.1007/978-3-540-72865-8_15
[23] V. Perebeinos, J. Tersoff, P. Avouris. Nano Lett., **6**, 205 (2006). https://doi.org/10.1021/nl052044h
[24] T. Dürkop, S.A. Getty, E. Cobas, M.S. Fuhrer. Nano Lett., **4**, 35 (2004). https://doi.org/10.1021/NL034841Q
[25] M. Shur. *Physics of Semiconductor Devices* (Prentice Hall, 1990).
[26] C. Schönenberger, A. Bachtold, C. Strunk, J.P. Salvetat, L. Forró. Appl. Phys. A: Mater. Sci. Process., **69**, 283 (1999). https://doi.org/10.1007/s003390051003
[27] B. Stojetz, C. Hagen, C. Hendlmeier, E. Ljubović, L. Forró, C. Strunk. New J. Phys., **6**, 27 (2004). https://doi.org/10.1088/1367-2630/6/1/027
[28] J.F. Dayen, T.L. Wade, M. Konczykowski, J.E. Wegrowe, X. Hoffer. Phys. Rev. B, **72**, 073402 (2005). https://doi.org/10.1103/PHYSREVB.72.073402
[29] R. Jago, R. Perea-Causin, S. Brem, E. Malic. Nanoscale, **11**, 10017 (2019). https://doi.org/10.1039/c9nr01714c
[30] E. Decrossas, M.A. El Sabbagh, V.F. Hanna, S.M. El-Ghazaly. IEEE Trans. Electromagn. Compat., **54**, 81 (2012). https://doi.org/10.1109/TEMC.2011.2174788
[31] J. Wu, L. Kong. Appl. Phys. Lett., **84**, 4956 (2004). https://doi.org/10.1063/1.1762693
[32] J.M. Marulanda, A. Srivastava. Phys. Status Solidi B, **245** (11), 2558 (2008). https://doi.org/10.1002/PSSB.200844259
[33] R.S. Lee, H.J. Kim, J.E. Fischer, A. Thess, R.E. Smalley. Nature, **388**, 255 (1997). https://doi.org/10.1038/40822
[34] M. Radosavljević, J. Appenzeller, P. Avouris, J. Knoch. Appl. Phys. Lett., **84**, 3693 (2004). https://doi.org/10.1063/1.1737062
[35] L. Duclaux. Carbon (N.Y.), **40**, 1751 (2002). https://doi.org/10.1016/S0008-6223(02)00043-X
[36] M. Shur. *GaAs devices and circuits* (Plenum Press, N.Y., 1987).
[37] J. Li, Q. Ye, A. Cassell, H.T. Ng, R. Stevens, J. Han, M. Meyyappan. Appl. Phys. Lett., **82**, 2491 (2003). https://doi.org/10.1063/1.1566791
[38] B. Kim, M.L. Geier, M.C. Hersam, A. Dodabalapur. Sci. Rep., **7**, 39627 (2017). https://doi.org/10.1038/srep39627
[39] Q. Bao, K.P. Loh. ACS Nano, **6**, 3677 (2012). https://doi.org/10.1021/NN300989G
[40] Y. Zhou, A. Gaur, S.H. Hur, C. Kocabas, M.A. Meitl, M. Shim, J.A. Rogers. Nano Lett., **4**, 2031 (2004). https://doi.org/10.1021/nl048905o
[41] A.I. Vorobyova. Uspekhi fiz. nauk, **179**, 243 (2009). (in Russian).
[42] R. Rosen, W. Simendinger, C. Debbault, H. Shimoda, L. Fleming, B. Stoner, O. Zhou. Appl. Phys. Lett., **76**, 1668 (2000). https://doi.org/10.1063/1.126130

Translated by Ego Translating